Simulation of Deuterium Retention in Tungsten Exposed to Divertor Plasmas*)

Kaoru OHYA and Yoshio SONEDA

Institute of Technology and Science, The University of Tokushima, Tokushima 770-8506, Japan

To study tritium retention in a divertor target made of tungsten, thermal processes of hydrogen isotopes, including implantation, diffusion, trapping and detrapping, and surface recombination, are modeled for ITER plasma configuration. The material parameters governing the processes are estimated by simulating an existing TDS experiment by using the model. In case of the inner target, dominant retention mechanism is the trapping in the deep trap and most of the T atoms are kept in the trap even after discharge. Mobile T atoms dominate the T retention in the outer target due to its high temperature, the amount of which is ten times greater than that in the inner target. The T retention after a discharge of 400 s is estimated to be tens of mg, resulting in 10000 or more discharges after which a T safety limit of 700 g is reached. Nevertheless, it strongly depends on the trap concentration in the target.

1. Introduction

Tritium (T) retention in the vessel wall of ITER must be limited for safety reasons. Dominant retention mechanism for the divertor target made of tungsten (W) is implantation. Implanted T atoms are thermalized after frequent collisions and then diffuse deeper into the target. Hydrogen isotope atoms are highly mobile at elevated temperatures and they are trapped in radiation damage sites or defects of the target [1]. In the present study, such thermal processes of implanted deuterium (D) atoms in a W target are modeled for an ITER plasma configuration. The time evolution of the T retention during and after a discharge is calculated, so that the retained amount of T within a discharge is estimated for the inner and outer regions.

2. Models for Deuterium Retention in Tungsten

The thermal processes of implanted D atoms are treated by a one-dimensional diffusion equation with implantation, trapping and detrapping terms in the same way as the DIFFUSE code [2]. The diffusivity is assumed to be independent of depth, so that $D = D_0 \exp(-E_D/kT)$, where E_D and T are the activation energy for diffusion and the target temperature, respectively. For the trapping term, we assume two types of traps with different detrapping energies, E_{T1} and E_{T2}. Surface recombination is assumed to take place with the rate coefficient of Pick type [3], $K_r = K_{r0} T^{-1/2} \exp(-E_r/kT)$, so that the released D flux is calculated by multiplying K_r with the density of mobile D

atoms at the surface, leading to the boundary condition.

The surface layer of the target is divided into 1500 slabs of constant thickness of 100 nm. Collision process of implanted particles and the depth profile after the process are calculated using a binary collision approximation (BCA) code, EDDY [4], with 10^4 pseudo particles, each representing a differential fluence $\Delta\Phi$. The profile is used as input for the diffusion equation with the diffusion time of 1 s so that $\Delta\Phi = \Gamma$, where Γ is the flux of implanted particles. The depth profile after diffusion is subject to implantation with the next $\Delta\Phi$. In this calculation, the implantation profile is the same as the first one although in reality the profile will be changed. This sequence is performed N times to simulate the time evolution of particle retention and release during long time, N s, like as 1000 s or more.

3. Parameter Fitting with a TDS Experiment

The time evolution of the D flux released from a W surface is calculated to compare with a thermal desorption spectroscopy (TDS) experiment [5]. In the experiment, a wrought W target was irradiated by D_3^+ ions with an energy of 100 eV/D and a flux of 2.5×10^{15} cm^{-2}s^{-1}. The target was kept at room temperature in the ion implantation phase (~400 s) and in the successive outgassing phase (~300 s) without implantation before heating within the TDS phase at a rate of about 5 K/s. In this condition, the reflection coefficient of incident ions is high (~0.59). The reflected particles are neutralized in the target, a low-energy part of which contribute to the released D flux. Therefore, the re-
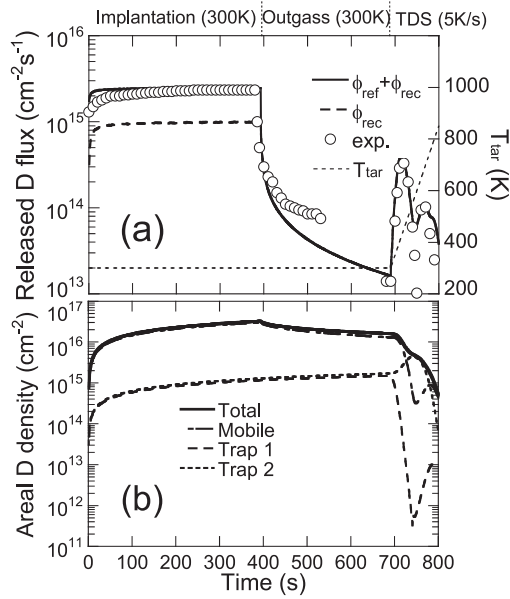
Fig. 1 (a) Temporal variations of the sum of reflection flux (ϕ_{ref}) and recombination flux (ϕ_{rec}) from W and (b) the areal densities of mobile and trapped D atoms during 300 eV D_3^+ ion irradiation, during isothermal release and during thermal desorption. T_{tar} is the target temperature.

Table 1   Material parameters used for simulation.

(a) Diffusion		(b) Surface recombination	
D_0 (cm^{2}s^{-1})	E_D (eV)	E_r (eV)	K_r (cm^{4}K$^{1/2}$s^{-1})
0.39	2.5×10^{-7}	–0.59	1.2×10^{-25}

(c) Trapping			
E_{T1} (eV)	D_{trap1}/W	E_{T2} (eV)	D_{tarp2}/W
0.85	0.001	1.5	0.001

flected flux is added to the recombination flux in order to obtain total flux of released D atoms, being compared with the measured flux. The best fitted change in the released flux, defined by the sum of reflection and recombination fluxes, is shown in Fig. 1 (a) along with the observed one. The material parameters used for simulation are listed in Table 1. The activation energy E_D is taken from [5, 6] and the pre-exponential factor D_0 is determined by fitting the flux change at the outgassing phase. For surface recombination, the activation energy and the pre-exponential factor are larger and smaller, respectively, than the reference values of -2.06 eV and 3.0×10^{-25} cm^{4}K$^{1/2}$s^{-1}, respectively [3], such that the rate coefficient K_r is comparable to that with other works [7,8]. Although the detrapping energies are approximately the same values as those (E_{T1} = 0.85 eV and E_{T2} = 1.4 eV) used in [5], the energy for the deeper trap is adjusted to E_{T2} = 1.5 eV to improve the agreement with the observed peaks in the TDS phase. The trap concentrations, D_{trap1}/W and D_{trap2}/W, and the target temperature, T_{tar}, are assumed to be uniform in the target, including the surface, and then, they are invariable during ion bombardment.

In Fig. 1 (b), the time evolution of the areal density of D atoms trapped in W is shown along with that of the density retained as mobile atoms. The density of mobile and trapped D atoms increases successively during implantation. After implantation, a part of mobile D atoms are released due to surface recombination. In contrast, trapped D atoms are kept to be retained in the target and they are detrapped when the target temperature rises during the TDS phase. At the early stage of the TDS phase with low target temperature, D atoms in the Trap 1 with low E_{T1} are released via mobile D atoms. At the delayed stage with higher temperature, D atoms in the deeper trap (Trap 2) are released.

4. Deuterium Retention in a Tungsten Target in a Divertor of ITER

D retention characteristics for inner and outer divertor targets, made of W, are studied in a detached plasma condition of ITER. The plasma parameters in front of the targets are taken from a B2-EIRENE calculation [9]. Figure 2 (a) shows a schematic view of the divertor region with the inner and outer targets and the divertor plasma. The input parameters used for simulation are shown in Figs. 2 (b) and 2 (c) for the inner and outer divertors, respectively, as a function of the distance from the strike point on the target. Using velocities of D ions along magnetic field lines and the angles intersecting the targets, the flux distribution along the target is calculated. The mean impact energy is $E = 2T_i + 3T_e$, where T_i and T_e are the local ion and electron temperatures. The magnetic field lines intersect the targets at very shallow angles between $1°$ and $3°$, where the gyro-motion and sheath electric field influence the angle of incidence. Therefore, the angular distribution of the ions is calculated at different magnetic field angles using a particle-in-cell simulation [10]. The average angle of the distribution, depending on the magnetic angle at each position on the target, are $12°\sim18°$, which are used as incident angles. The energy of D ions exposed to the targets is mostly tens of eV or less and the angle of incidence is shallow. In the cases, the BCA code, such as EDDY, overestimates the implantation flux to the target due to lack of many body effect. Using a molecular dynamics simulation [11], the sticking coefficient is estimated to be $0.01\sim0.02$, slightly depending on the target temperature, in the relevant energy and angle ranges. Therefore, it is assumed to be 0.01 for the present calculation of the implantation flux. The temperature depending on the position on the target is taken from [12], where the temperature were calculated assuming CFC, not W, with the thickness of 10 mm. Typical duration of a discharge in ITER is 400 s. The target temperature at each position is kept constant after discharge as well as during it. The temperature gradient along the inner and outer targets is not taken into account for our calculation, so that D atoms can diffuse in depth.

The fitted material parameters in Table 1 are used. The
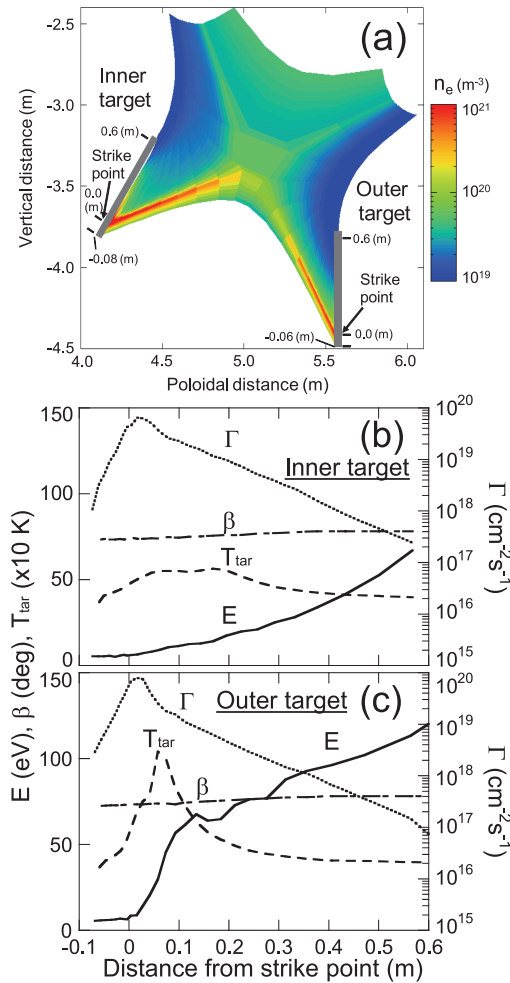
Fig. 2 (a) Schematic view of the divertor region of ITER with inner and outer targets, along with the electron density distribution in the divertor plasma, calculated by B2-EIRENE [9]. Incident energy (E), angle (β) and flux (Γ) and target temperature (T_{tar}) as a function of the position on the inner and outer targets are shown in (b) and (c), respectively. The angle is measured from the surface normal.

trap concentration strongly depends on the material and additional traps may be produced in the near-surface region due to high D fluxes to the target, resulting in a depth-dependent concentration. Therefore, parameter studies are also done for the trap concentration.

Figures 3 (a) and 3 (b) shows the profiles of D atoms retained along the inner and outer targets, respectively, just after a discharge (400 s) and subsequently after it (1000 s). The profiles are dominated by the target temperature at each position. At the position where the temperature is high, the number of retained D atoms increases continuously up to 400 s without any saturation. Due to frequent detrapping from the traps and subsequent thermal diffusion, most of D atoms are retained as mobile atoms and they are distributed deeper and deeper. On the other hand, at the low temperature position, it tends to saturate where
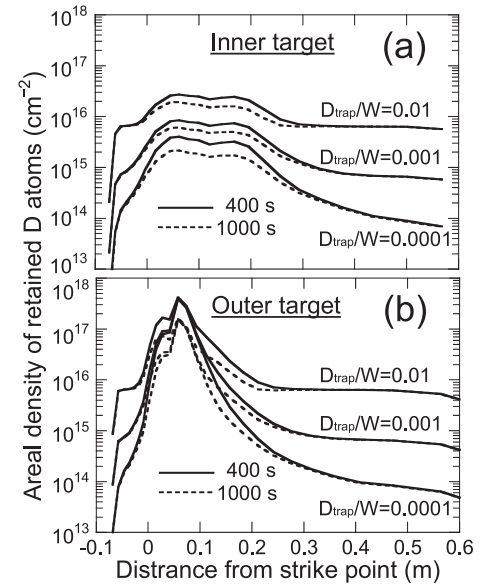
Fig. 3 Areal density profiles of retained D atoms along the inner target (a) and outer target (b) with different trap concentration, D_{trap}/W, just after and subsequently after discharge.

most of trap sites near the surface are occupied by implanted D atoms. After discharge (1000 s), a part of mobile D atoms retained are released due to surface recombination, however, most of D atoms are kept to be retained in the target, where they can diffuse deeper. Also as shown in Figs. 3 (a) and 3 (b), the number of retained D atoms at the low temperature position strongly depends on the trap concentration in W. At the position with high temperature, a weaker dependence is obtained due to dominant retention of mobile atoms.

5. Tritium Retention in Vessel Walls of ITER

From the distribution of retained D atoms during and after discharge, the T retention in the inner and outer targets are estimated by taking the atomic mass difference between D and T into account, and assuming toroidal symmetry. Figures 4 (a) and 4 (b) show the results along with partial retentions in two types of traps distinguished from that of mobile T atoms. In case of the inner target, dominant retention mechanism is the trapping in the deep trap (Trap 2) during discharge and most of the T atoms are kept in the trap even after discharge. On the other hand, mobile T atoms dominate the T retention in the outer target due to its high temperature leading to detrapping from the trap and subsequent diffusion inside the target. The T atoms are retained ten times more in the outer target than in the inner target during discharge, whereas sufficiently after discharge the T retention is reduced due to surface recombination of mobile atoms.

Due to dominant T trapping in the deeper traps, the T retention in the inner target is strongly enhanced due to an
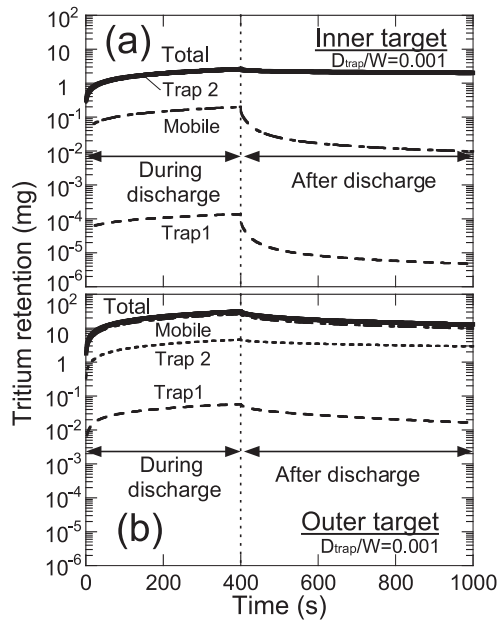
Fig. 4 Time evolution of T retention for the inner target (a) and outer target (b) during and after discharge, along with the contributions of mobile and trapped atoms to it.
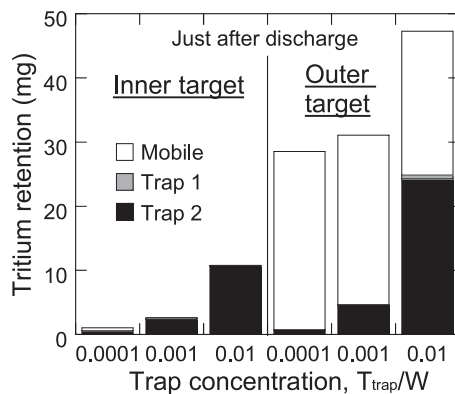
Fig. 5 T retention in the inner and outer targets just after discharge as a function of the trap concentration, along with the contributions of mobile and trapped atoms to it.

increase in the trap concentration as shown in Fig. 5 where the T retention is calculated just after a discharge (400 s). For the highest concentration ($T_{trap}/W = 0.01$), the T retention in the inner target approaches the values in the outer target, decreasing with time after discharge. Finally, the

number of discharges, after which an in-vessel T safety limit of 700 g is reached, is estimated from the sum of T retention of the inner and outer targets. The T retention in other wall components such as upper baffle and dome, made of W, and a first wall made of beryllium (Be) is not taken into account. The number of discharges is of the range between 12000 and 24000, depending on the trap concentration from 0.01 to 0.0001. It is increased to the values between 22000 and 60000, if the T retention sufficiently after discharge (1000 s) is used.

6. Concluding Remarks

Dominant retention mechanism for the inner target is the trapping in the deep trap and most of the retained T atoms are kept in the trap even after discharge. Mobile T atoms dominate the T retention in the outer target due to its high temperature, leading to detrapping from the trap and subsequent diffusion in the target. The T retention after a discharge duration of 400 s is estimated to be tens of mg, strongly depending on the trap concentration in the target. It results in 10000 discharges or more after which a T safety limit of 700 g is reached. Nevertheless, Be used for the first wall is strongly eroded due to its low surface binding energy and a portion of eroded Be atoms migrates towards the divertor targets, although most of atoms redeposit on the other areas of the first wall. Codeposition mechanism for the Be deposits may dominate the T retention in the W target in both inner and outer regions.

[1] T. Tanabe et al., J. Nucl. Mater. **196-198**, 11 (1992).
[2] K.L. Wilson et al., J. Nucl. Mater. **76/77**, 291 (1978).
[3] M.A. Pick et al., J. Nucl. Mater. **131**, 208 (1985).
[4] K. Ohya, Phys. Scr. **T124**, 70 (2006).
[5] C. Garcia-Rosales et al., J. Nucl. Mater. **233-237**, 803 (1996).
[6] T. Ono et al., J. Nucl. Mater. **390-391**, 713 (2009).
[7] R.A. Anderl et al., Fusion Technol. **21**, 745 (1992).
[8] W.R. Wampler, J. Nucl. Mater. **145-147**, 313 (1987).
[9] G. Federici et al., J. Nucl. Mater. **313-316**, 11 (2003).
[10] K. Inai et al., J. Plasma Fusion Res. SERIES **8**, 433 (2009).
[11] K. Ohya et al., J. Nucl. Mater. **417**, 637 (2011).
[12] G. Federici et al., Plasma Phys. Control. Fusion **45**, 1523 (2003).